Measurement of electron paramagnetic resonance using terahertz time-domain spectroscopy

Kohei Kozuki, Takeshi Nagashima,* and Masanori Hangyo

Institute of Laser Engineering, Osaka University, Suita, Osaka 565-0871, Japan
nagasima@ile.osaka-u.ac.jp

Abstract: We present a frequency-domain electron spin resonance (ESR) measurement system using terahertz time-domain spectroscopy. A crossed polarizer technique is utilized to increase the sensitivity in detecting weak ESR signals of paramagnets caused by magnetic dipole transitions between magnetic sublevels. We demonstrate the measurements of ESR signal of paramagnetic copper(II) sulfate pentahydrate with uniaxial anisotropy of the g-factor under magnetic fields up to 10 T. The lineshape of the obtained ESR signals agrees well with the theoretical predictions for a powder sample with the uniaxial anisotropy.

OCIS codes: (300.6495) Spectroscopy, terahertz; (260.2130) Ellipsometry and polarimetry; (300.6500) Spectroscopy, time-resolved.

References and links

1. For text, A. Abragam and B. Bleaney, *Electron Paramagnetic Resonance of Transition Metal Ions* (Clarendon Press, 1970).
2. K. Möbius, A. Savitsky, A. Schnegg, M. Plato, and M. Fuchst, "High-field EPR spectroscopy applied to biological systems: characterization of molecular switches for electron and ion transfer," Phys. Chem. Chem. Phys. **7**(1), 19–42 (2005).
3. M. Bennati and T. F. Prisner, "New developments in high field electron paramagnetic resonance with applications in structural biology," Rep. Prog. Phys. **68**(2), 411–448 (2005).
4. H. Hachisuka, K. Awaga, T. Yokoyama, T. Kubo, T. Goto, and H. Nojiri, "Structure and magnetic properties of the single-molecule magnet $[Mn_{11}CrO_{12}(O_2CCH_3)16(H_2O)4]\cdot 2CH_3COOH\cdot 4H_2O$: magnetization manipulation and dipolar-biased tunneling in a Mn11Cr/Mn12 mixed crystal" Phys. Rev. B **70**(10), 104427 (2004).
5. M. Yoshida, K. Shiraki, S. Okubo, H. Ohta, T. Ito, H. Takagi, M. Kaburagi, and Y. Ajiro, "Energy structure of a finite Haldane chain in $Y_2BaNi_{0.96}Mg_{0.04}O_5$ studied by high field electron spin resonance," Phys. Rev. Lett. **95**(11), 117202 (2005).
6. S. A. Zvyagin, M. Ozerov, E. Cizmár, D. Kamenskyi, S. Zherlitsyn, T. Herrmannsdörfer, J. Wosnitza, R. Wünsch, and W. Seidel, "Terahertz-range free-electron laser electron spin resonance spectroscopy: techniques and applications in high magnetic fields," Rev. Sci. Instrum. **80**(7), 073102 (2009).
7. L. Mihály, D. Talbayev, L. F. Kiss, J. Zhou, T. Fehér, and A. Jánossy, "Field-frequency mapping of the electron spin resonance in the paramagnetic and antiferromagnetic states of $LaMnO_3$," Phys. Rev. B **69**(2), 024414 (2004).
8. F. El Hallak, J. van Slageren, J. Gómez-Segura, D. Ruiz-Molina, and M. Dressel, "High-frequency ESR and frequency domain magnetic resonance spectroscopic studies of single molecule magnets in frozen solution," Phys. Rev. B **75**(10), 104403 (2007).
9. N. Kida, Y. Takahashi, J. S. Lee, R. Shimano, Y. Yamasaki, Y. Kaneko, S. Miyahara, N. Furukawa, T. Arima, and Y. Tokura, "Terahertz time-domain spectroscopy of electromagnons in multiferroic perovskite manganites," J. Opt. Soc. Am. B **26**(9), A35–A51 (2009).
10. Y. Ikebe and R. Shimano, "Characterization of doped silicon in low carrier density region by terahertz frequency Faraday effect," Appl. Phys. Lett. **92**(1), 012111 (2008).
11. Y. Ikebe and R. Shimano, "Characterization of doped silicon in low carrier density region by terahertz frequency Faraday effect: erratum," Appl. Phys. Lett. **92**, 149901 (2008).
12. F. Bloch, "Nuclear Induction," Phys. Rev. **70**(7-8), 460–474 (1946).
13. R. D. Arnold and A. F. Kip, "Paramagnetic resonance absorption in two sulfates of copper," Phys. Rev. **75**(8), 1199–1205 (1949).
14. H. Ohta, N. Yamauchi, T. Nanba, M. Motokawa, S. Kawamata, and K. Okuda, "EPR and AFMR of Li_2CuO_2 in submillimeter wave region," J. Phys. Soc. Jpn. **62**(2), 785–792 (1993).
15. M. Born and E. Wolf, *Principles of Optics* (Cambridge University Press, 1999), Chap. 1.6.

#155611 - $15.00 USD Received 30 Sep 2011; revised 3 Nov 2011; accepted 7 Nov 2011; published 22 Nov 2011

16. J. Krzystek, A. Sienkiewicz, L. Pardi, and L. C. Brunel, "DPPH as a Standard for High-Field EPR," J. Magn. Reson. **125**(1), 207–211 (1997).
17. J. van Tol, L.-C. Brunel, and R. J. Wylde, "A quasioptical transient electron spin resonance spectrometer operating at 120 and 240 GHz," Rev. Sci. Instrum. **76**(7), 074101 (2005).

1. Introduction

Electron spin resonance (ESR) is a useful tool for material analysis in various fields including physics, chemistry, and biology. When the applied magnetic field B and the angular frequency ω of radiation transmitted through a paramagnetic sample with negligible interaction between electron spins satisfy $\hbar\omega = g\mu_B B$ (where $\hbar$ is the reduced Planck constant; μ_B, the Bohr magneton; and g, the g-factor), resonant absorption of the radiation occurs [1]. The resonance condition is modified by total spin angular momentum, anisotropy, interaction between electron spins, magnetic field-induced transitions, and so on. Thus, knowledge of B and ω at resonances provides abundant information on the electronic state and microscopic structure around atoms associated with the electron spins.

ESR using X-band microwaves (~10 GHz) is a well-established technique. Recently, ESR measurements at terahertz frequencies (THz-ESR) have attracted much attention [2–9]. By THz-ESR, the resolution of electron paramagnetic resonance measurements should be improved, thus enabling signals from slightly different g-factors to be separated [2,3]. THz-ESR allows for high and/or integer spin systems with large zero-field splitting to be investigated [4–6].

In conventional ESR measurements, an applied magnetic field is continuously varied while the frequency of a monochromatic radiation source is fixed. In such a scheme, to detect resonances with zero-field splitting, the radiation source with the frequency close to the zero-field splitting has to be used. However, it is difficult to select an appropriate frequency of the radiation source when the magnitude of the zero-field splitting of materials is unknown. In contrast, using a spectroscopic technique, the resonances with unknown zero-field splitting can be observed if the radiation source has a sufficient broadband spectrum. Thus, frequency-domain ESR is needed for investigating those resonances [7–9]. In addition, field-frequency maps [4,5,7,8], which provide abundant information of spin structures, are more easily obtained by frequency-domain ESR compared with conventional ESR where the radiation source must be replaced to change the frequency [4,5].

In this article, we report the development of a frequency-domain ESR measurement system using terahertz time-domain spectroscopy (THz-TDS) for analyzing paramagnetic materials. A crossed polarizer technique is utilized to increase the sensitivity in detecting weak ESR signals. We show the validity of the developed system by measuring an ESR standard material. The proposed ESR measurements using subpicosecond terahertz pulses represent progress toward realizing time-resolved ESR with extremely high time-resolution.

2. Principle of measurements and setup

ESR signals originate from the absorption of a circularly polarized wave via magnetic dipole transitions between magnetic sublevels. The ESR absorption of paramagnetic materials, however, is too small to detect with conventional transmission measurements using THz-TDS. As shown in Fig. 1(a), a circularly polarized component at ESR frequencies is absorbed. This results in the induction of polarization perpendicular to the incident linearly polarized wave. In this work, to detect ESR signals from paramagnets, crossed polarization at resonance frequencies induced by the absorption of the circularly polarized wave is detected by means of a pair of crossed wire grid polarizers [10,11]. Since this scheme is a null method, the sensitivity of the detection can be increased, thus enabling crossed polarization with small amplitude to be measured.

A schematic diagram of the experimental setup is shown in Fig. 1(b). A superconducting magnet that generates 10 T at maximum is installed in a conventional THz-TDS system. Photoconductive antennas excited by optical pulses (center wavelength, 780 nm; duration, 98 fs; repetition rate, 50 MHz; average power, 12 mW) were used as the emitter and detector of

#155611 - $15.00 USD Received 30 Sep 2011; revised 3 Nov 2011; accepted 7 Nov 2011; published 22 Nov 2011

THz pulses. Free-standing wire grids (Specac) with a wire diameter of 5 μm, a spacing of 12.5 μm, and a nominal cutoff frequency of ~6 THz were used as a polarizer (WG1) and an analyzer (WG2). The wires of WG1 were set perpendicular to those of WG2. For better sensitivity in detecting the crossed polarization, stacks of two wire grids were used in WG1 and WG2. The THz pulse waveform $E_s(t)$ with polarization orthogonal to that of pulses incident on the samples were measured in the experiments.

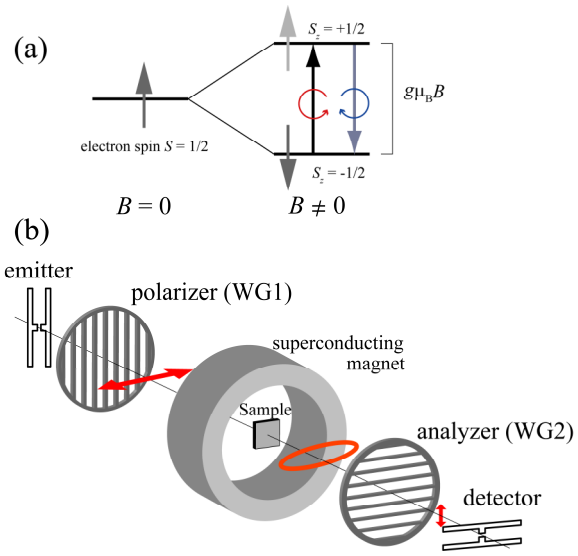

Fig. 1. (a) Schematic diagram of absorption and emission of circularly polarized electromagnetic waves caused by magnetic dipole transitions between magnetic sublevels. (b) Schematic diagram of experimental setup.

Here, we define the ESR signal as $|E_s(\omega)/E_0(\omega)|$, where $E_s(\omega)$ and $E_0(\omega)$ are the complex amplitude spectra deduced from the waveforms of the crossed polarization ($E_s(t)$) and incident THz waves ($E_0(t)$) by complex Fourier transformation. The linearly polarized incident wave can be viewed as a superposition of right- and left-handed circularly polarized waves with complex amplitude $E_0(\omega)/2$. $E_s(\omega)$ in magnetic field B is described by

$$E_s = iE_0(t_- - t_+)/2, \tag{1}$$

where t_+ and t_- are the complex amplitude transmittance spectra of the left- and right-handed circularly polarized waves, respectively. When interference from multiply reflected THz waves in a sample is ignored, t_+ and t_- are given by

$$t_\pm = \frac{4Z_\pm}{(Z_\pm + 1)^2} e^{-ik_0 n_\pm d}, \tag{2}$$

where k_0 is the wavenumber of THz wave in free space, d is the thickness of the sample, and $Z_\pm = (\mu_\pm/\varepsilon)^{1/2}$ and $n_\pm = (\mu_\pm \varepsilon)^{1/2}$ are the complex impedance and complex refractive index for the circularly polarized waves, respectively. The dielectric constant ε is assumed to be a real constant independent of ω and B, which is reasonable in insulating paramagnets used in this study. $\mu_\pm = \mu'_\pm - i\mu''_\pm$ are the complex permeability for the circularly polarized waves. For paramagnets, $\mu'_\pm \sim 1$ and $\mu''_\pm << 1$ hold due to their weak magnetic response. Considering above approximations, Eq. (1) reduces to $E_s / E_0 \propto \omega(\chi''_+ - \chi''_-)d$, where $\chi''_\pm$ are the imaginary parts of the complex magnetic susceptibility $\chi_\pm = \chi'_\pm - i\chi''_\pm$ for the circularly polarized waves having the relation of $\mu'_\pm - i\mu''_\pm = 1 + 4\pi\chi'_\pm - i4\pi\chi''_\pm$. Under the condition that

#155611 - $15.00 USD Received 30 Sep 2011; revised 3 Nov 2011; accepted 7 Nov 2011; published 22 Nov 2011

the magnetic field of the THz pulses is sufficiently weak, the expressions for $\chi'_{\pm}$ and $\chi''_{\pm}$ derived from the Bloch equations [12] are

$$\chi_{\pm}' = \frac{1}{2}\chi_0\omega_0 \frac{(\omega_0 \mp \omega)}{d\omega^2 + (\omega_0 \mp \omega)^2} \quad and \quad \chi_{\pm}'' = \frac{1}{2}\chi_0\omega_0 \frac{d\omega}{d\omega^2 + (\omega_0 \mp \omega)^2}, \qquad (3)$$

respectively, where χ_0 is the static magnetic susceptibility, $\omega_0 = g\mu_B B/\hbar$ is the resonance angular frequency, and $d\omega$ is the inverse of the transverse relaxation time T_2. Using the absorption coefficients $\alpha_{\pm} \propto \omega\varepsilon\chi''_{\pm}$ for the circularly polarized waves, we obtain $E_s / E_0 \propto (\alpha_+ - \alpha_-)d$, which means that $|E_s(\omega)/E_0(\omega)|$ corresponds to lineshape of the ESR absorption at frequencies near the resonances. Thus, $|E_s(\omega)/E_0(\omega)|$ is defined as the ESR signal in this study.

3. Experiments

The validity of the proposed scheme is investigated by measuring Copper(II) sulfate pentahydrate ($CuSO_4 \cdot 5H_2O$), which is an ESR standard material as samples. Powder of the material was pressed to obtain disks (diameter, 13 mm; thickness, ~2 mm; mass, 566 mg). Waveforms of E_s were recorded up to ~800 ps. Thus, the frequency resolution of deduced ESR signals was ~1.25 GHz. The waveforms shown in this article are averages of 50 scans. All measurements were carried out at room temperature.

First, the crossed polarization waveforms in magnetic fields with positive and negative polarities were measured. Oscillations with a period of ~3 ps induced by ESR were observed in the waveforms in ± 10 T fields (inset, Fig. 2(a)). When the polarity of the applied magnetic field is reversed, the helicity of the dominantly absorbed circular polarization is switched, which results in the polarity reversal of $E_s(t)$. On the waveforms, there are small artifacts that originate from leakage of the incident polarization caused by the low extinction ratios of the wire grids. The phase of those components remains the same when the direction of the magnetic field is reversed. According to Refs. 10 and 11 signals induced by only ESR can be extracted by subtracting $E_s(t)$ in negative magnetic field $-B$ from that in positive magnetic field $+B$. In Fig. 2(a), the extracted waveform ($[E_s(t, B = +10\text{ T}) - E_s(t, B = -10\text{ T})]/2$) is shown by the solid curve.

4. Results and discussions

The spectrum of the ESR signal deduced from the extracted waveform in a 10 T field is displayed in Fig. 2(b). The absolute value of ESR signal $|E_s(\omega)/E_0(\omega)|$ is ~3.7×10^{-3} at 0.29 THz where a prominent peak is observed. $CuSO_4 \cdot 5H_2O$ has uniaxial anisotropy of the g-factor, owing to the tetragonal crystal field around Cu^{2+} ions with $S = 1/2$. The g-factors with magnetic fields parallel and perpendicular to the tetragonal axis have been reported to be $g_{//} = 2.38$ and $g_{\perp} = 2.05$, respectively [13]. The effective magnetic susceptibility χ_{eff} of a powder sample with uniaxial anisotropy is given by

$$\chi_{eff}(\omega) = \int_0^{\frac{\pi}{2}} \chi_{dist}(\omega, \theta) \sin\theta \, d\theta, \qquad (4)$$

where θ is the angle between the tetragonal axis and the magnetic field and χ_{dist} is the distribution function of the complex magnetic susceptibility obtained from $\chi_{\pm}$ by replacing ω_0 in Eq. (2) with [14]

#155611 - $15.00 USD Received 30 Sep 2011; revised 3 Nov 2011; accepted 7 Nov 2011; published 22 Nov 2011

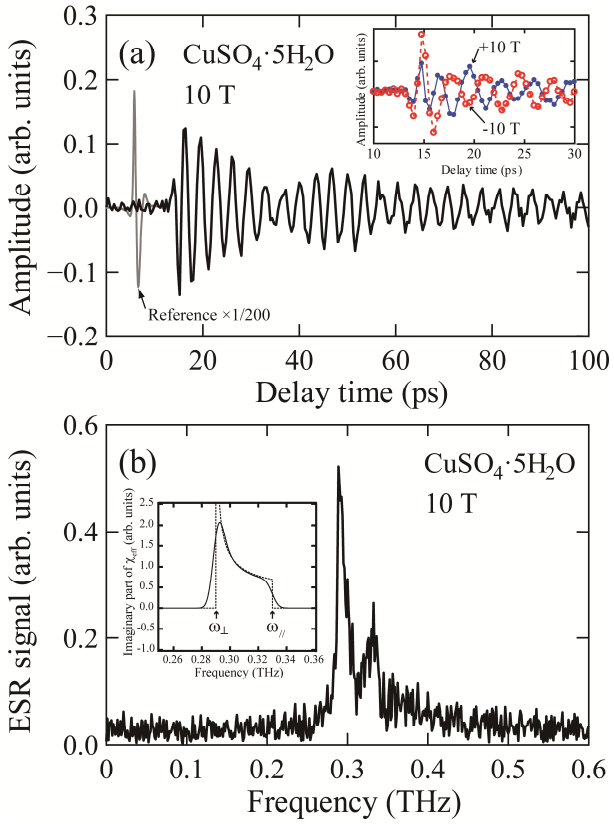

Fig. 2. (a) Waveform of crossed polarization induced by ESR. Solid curve shows the waveform extracted by subtracting the waveform of the crossed polarization induced in $CuSO_4 \cdot 5H_2O$ in a −10 T field from that in a + 10 T field. Waveforms in ± 10 T fields are shown by solid and open circles, respectively, in the inset. Waveform of the incident THz pulses is shown by the gray curve for comparison. (b) ESR spectrum of $CuSO_4 \cdot 5H_2O$. Inset shows a typical spectrum of the imaginary part of the effective magnetic susceptibility.

$$\omega(\theta) = \frac{\mu_B}{\hbar} B \sqrt{g_{//}{}^2 \cos^2\theta + g_{\perp}{}^2 \sin^2\theta}. \tag{5}$$

A typical lineshape of the imaginary part of χ_{eff} that corresponds to the ESR signal is schematically shown in the inset of Fig. 2(b). A peak and a discontinuity, respectively, are expected at angular frequencies around $\omega_{\perp,//} = g_{\perp,//}\,\mu_B B/\hbar$. The ESR signal in a 10 T field (Fig. 2(b)) appears to be consistent with the expected results. However, the lineshape of the ESR signals depends on the applied magnetic field and on the sample thickness as shown by the solid curves in Fig. 3(a) and 3(b), respectively. This is attributed to interference effects of multiply reflected THz waves in the samples used in this study, which were parallel plates. Here, we calculate the ESR signals $|E_s(\omega)/E_0(\omega)|$ as follows. Taking into account the interference effects of the THz waves, the complex amplitude transmittance of the parallel plate with thickness d is expressed by [15]

$$\tilde{t}(\omega) = \frac{t_{01}t_{10}e^{-in\omega d/c}}{1 - r_{10}{}^2 e^{-i2n\omega d/c}}, \tag{6}$$

#155611 - $15.00 USD Received 30 Sep 2011; revised 3 Nov 2011; accepted 7 Nov 2011; published 22 Nov 2011

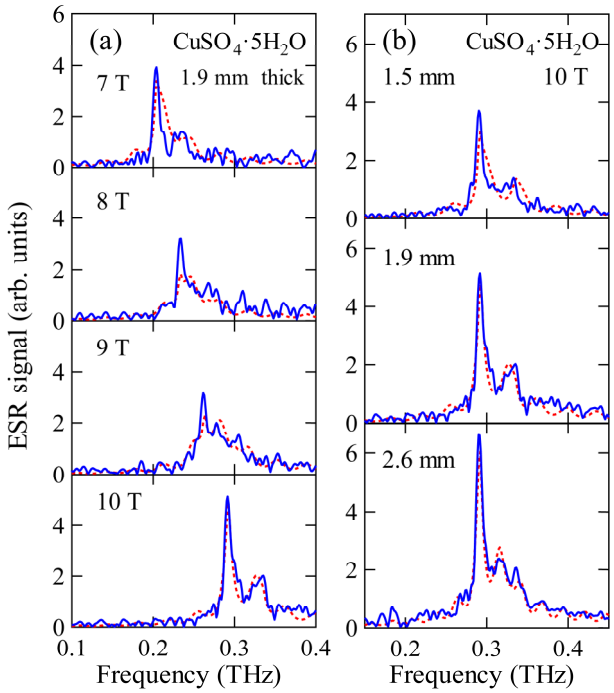

Fig. 3. ESR spectra of $CuSO_4 \cdot 5H_2O$ (a) with sample thickness of 1.9 mm in various magnetic fields and (b) with various sample thicknesses in a 10 T field. Results of experiments and calculations are shown by solid and dashed curves, respectively.

where $n = [\varepsilon (1 + \chi_{eff})]^{1/2}$ is the complex refractive index of the sample and $t_{01} = 2\ Z/(Z_0 + Z)$, $t_{10} = 2\ Z_0/(Z_0 + Z)$, and $r_{10} = (Z_0\text{-}Z)/(Z_0 + Z)$, where Z_0 and $Z = Z_0\ [(1 + \chi_{eff})/\varepsilon]^{1/2}$ are the impedances of vacuum and sample, respectively. $\varepsilon = 4.84\text{-}0.01i$ determined by transmission THz-TDS measurements without magnetic field is used in the calculations. Using χ_{eff} for the left- and right-handed circularly polarized waves, t_+ and t_- in Eq. (1) are calculated by using Eq. (6), and then $|E_s(\omega)/E_0(\omega)|$ is obtained. In the calculations, the parameters $d\omega \approx 11$ GHz, $g_{//} = 2.40$, and $g_\perp = 2.09$ are used, which are consistent with the previously reported values [13]. The measured ESR signals are reproduced well by the calculations shown by the dashed curves in Fig. 3. The interference effects mentioned above can be reduced using wedged-shaped samples.

The frequency resolution presented in this study is ~1.25 GHz, which is determined by the length of the delay stage used in THz-TDS. 2,2-diphenyl-1-picrylhydrazyl (DPPH), one of the ESR standard samples, is expected to have ESR absorption line with a linewidth of ~14 MHz at 10 T [16]. To resolve such narrow resonances, a delay stage with a length longer than several tens of meters is needed, which is unrealistic. One of the options to resolve the problem may be to use an asynchronous optical sampling technique with two sets of femtosecond pulse lasers operated at a repetition rate lower than ~10 MHz. Besides this, maximum entropy method may be used to obtain spectra with improved frequency resolution from measured waveforms with an ordinary delay stage.

Finally, we would like to point out a possibility of time-resolved ESR measurements with extremely high time resolution based on the system with a THz pulse source developed in this study. Time-resolved ESR is used to study the mechanisms of reaction processes since it can detect generated free radicals that induce paramagnetic ESR. However, the time resolution of conventional ESR systems is ~1 ns at best [17]. Thus, free radicals and excitation states with shorter lifetime in photoinduced reactions, such as photosynthesis reactions and photoinduced damage of DNA, have rarely been investigated by time-resolved ESR. Since the duration of

#155611 - $15.00 USD Received 30 Sep 2011; revised 3 Nov 2011; accepted 7 Nov 2011; published 22 Nov 2011

the THz pulses is on the order of sub-picoseconds, an ESR system with optical pump-THz pulse probe spectroscopy is expected to have substantially improved time resolution.

5. Summary

In summary, for analyzing paramagnetic materials, we developed a frequency-domain ESR technique using THz-TDS. The ESR signal of the powder samples of $CuSO_4 \cdot 5H_2O$ was measured. The lineshape of the obtained ESR signals agrees well with the theoretical predictions for a powder sample with uniaxial anisotropy. The proposed ESR measurement scheme using subpicosecond terahertz pulses paves the way for future realization of time-resolved ESR with extremely high time-resolution.

Acknowledgments

We thank Prof. S. Okubo in Kobe University for his helpful comments and discussions. This work was partially supported by KAKENHI 21656019.

#155611 - $15.00 USD Received 30 Sep 2011; revised 3 Nov 2011; accepted 7 Nov 2011; published 22 Nov 2011